

CT Perfusion for Early Response Evaluation of Radiofrequency Ablation of Focal Liver Lesions: First Experience

Herman P. Marquez¹ · Gilbert Puippe¹ · Rishi Philip Mathew¹ · Hatem Alkadhi¹ · Thomas Pfammatter¹ · Michael A. Fischer¹

Received: 12 April 2016 / Accepted: 1 August 2016 / Published online: 3 November 2016

© Springer Science+Business Media New York and the Cardiovascular and Interventional Radiological Society of Europe (CIRSE) 2016

Abstract

Purpose To investigate the value of perfusion CT (P-CT) for early assessment of treatment response in patients undergoing radiofrequency ablation (RFA) of focal liver lesions.

Methods and Materials 20 consecutive patients (14 men; mean age 64 ± 14) undergoing P-CT within 24 h after RFA of liver metastases ($n = 10$) or HCC ($n = 10$) were retrospectively included. Two readers determined arterial liver perfusion (ALP, mL/min/100 mL), portal liver perfusion (PLP, mL/min/100 mL), and hepatic perfusion index (HPI, %) in all post-RFA lesions by placing a volume of interest in the necrotic central (CZ), the transition (TZ), and the surrounding parenchymal (PZ) zone. Patients were classified into complete responders (no residual tumor) and incomplete responders (residual/progressive tumor) using imaging follow-up with contrast-enhanced CT or MRI after a mean of 57 ± 30 days. Prediction of treatment response was evaluated using the area under the curve (AUC) from receiver operating characteristic analysis.

Results Mean ALP/PLP/HPI of both readers were 4.8/15.4/61.2 for the CZ, 9.9/16.8/66.3 for the TZ and 20.7/29.0/61.8 for the PZ. Interreader agreement of HPI was fair for the CZ (intraclass coefficient 0.713), good for the TZ (0.813), and excellent for the PZ (0.920). For both readers, there were significant differences in HPI of the CZ and TZ between responders and nonresponders (both, $P < 0.05$).

HPI of the TZ showed the highest AUC (0.911) for prediction of residual tumor, suggesting a cut-off value of 76 %.

Conclusion Increased HPI of the transition zone assessed with P-CT after RFA might serve as an early quantitative biomarker for residual tumor in patients with focal liver lesions.

Keywords Liver metastasis · Hepatocellular carcinoma · Radiofrequency ablation · Perfusion imaging · Computed tomography

Introduction

Local ablation is considered a first-line treatment option for patients at early stages of hepatocellular carcinoma (HCC) [1] and a second-line treatment option for patients with metastatic liver lesions not suitable for surgical therapy [2]. Among the local ablation techniques, radiofrequency ablation (RFA) has become a popular option for several reasons: minimal invasiveness with acceptable morbidity, excellent local tumor control, favorable overall survival gain, and potential to combine with other treatment options within a multimodality approach [3]. The delivery of high-frequency alternating current through the electrodes results in the heating of the surrounding liver tissue caused for the friction energy generated by rapidly moving ions. This phenomenon leads to coagulative necrosis and consecutively cell death [4].

Residual tumor and tumor recurrence, which occurs more frequently compared to surgery in both HCC [5] and metastasis [6], are limitations of the technique and should be detected as early as possible in order to repeat RFA treatment or to adapt the treatment regime. Delayed

✉ Herman P. Marquez
hermanpaulo.marquezmazquiaran@usz.ch

¹ Department of Diagnostic and Interventional Radiology,
Institute of Diagnostic and Interventional Radiology,
University Hospital Zurich, 8091 Zurich, Switzerland

diagnosis is associated with peripheral regrowth and makes retreatment difficult due to unfavorable growth patterns [7].

At many institutions, imaging assessment of treatment response is performed approximately 1 month after the RFA procedure to avoid normal periablation enhancement to be mistaken with residual disease [8]. It has been shown that MRI offers a higher sensitivity than CT (89 vs. 44 %) in detecting residual disease at approximately 1 month after RFA [9]. However, MRI shows limited availability and usefulness in the direct postoperative setting due to magnet restrictions, small patient bore, and substantial longer imaging times [10].

Perfusion CT (P-CT) of the liver provides qualitative and quantitative information about hepatic (micro-)circulation by repetitive sampling of contrast media uptake to the liver parenchyma at high temporal resolution. Hepatic perfusion parameters obtained from quantitative analysis, especially the hepatic perfusion index (HPI), which is based on the relation between arterial and portal venous blood flow, were shown to be good biomarkers for the detection of neoplastic liver disease [11, 12], for the prediction of therapy response [13], and for the assessment of therapy response [14–16], always within at least 1 month after treatment.

Moreover, P-CT was shown to be a reproducible method for treatment assessment 1 month following RFA in HCC acting as an alternative to standard multiphase CT [17]. However, the diagnostic value of P-CT for early treatment assessment directly after RFA treatment remains unclear. The purpose of our study was to determine the value of P-CT for early assessment of treatment response in patients undergoing RFA of liver metastases and HCC.

Materials and Methods

This is a retrospective, single-center study including institutional review board approval. Written informed consent was waived for all patients.

Patients

A total of 20 consecutive patients (14 men; 6 women; mean age 64 ± 14 years; range 25–80 years), who were referred for P-CT after RFA of liver metastases ($n = 10/20$, 50 %) or HCC ($n = 10/20$, 50 %) between February 2012 and December 2013, were included in this study. All patients with HCC suffered from liver cirrhosis, whereas all patients with liver metastases showed no signs of cirrhosis. The diagnosis of HCC was based on liver biopsy in two patients and on specific imaging features in patients with chronic liver disease and liver cirrhosis (arterial enhancement and portal venous wash-out) as defined by the

AASLD [1, 18] in the other 8 patients. The diagnosis of liver metastases was based on multiparametric MRI with liver-specific contrast agent in the 10 patients of the metastasis group. Diffusion restriction and arterial rim enhancement along with lack of liver-specific contrast media uptake was considered specific for hypovascular metastases in patients with histopathological proven colorectal ($n = 6$), small bowel ($n = 1$), esophagus ($n = 1$), and pancreatic ($n = 1$) cancer. In one patient with histopathological proven renal cell cancer ($n = 1$), hypervascular metastases were present showing homogeneous arterial enhancement along with diffusion restriction and lack of liver-specific contrast media uptake.

In all patients, P-CT was performed directly after RFA, with a mean interval between RFA and P-CT of 13 ± 8.6 h (range 3–24 h). Response assessment of RFA treatment was performed according to clinical routine using multiphase contrast-enhanced CT in 5 patients and MRI in 15 patients with a mean imaging follow-up of 57 ± 30 days (range, 17–95 days). Response assessment was performed based on EASL imaging criteria [19], and patients were further subclassified into complete responders (complete response) and incomplete responders (partial response, stable disease, and progressive disease).

Perfusion CT Data Acquisition

All patients were examined with a 128-slice dual-source CT (SOMATOM Definition Flash, Siemens Healthcare, Forchheim, Germany), using the 4D dynamic spiral acquisition mode with variable pitch [20]. The scan volume was individually defined for each patient by a supervising radiologist on the obtained topogram in order to cover the entire liver. Scan protocol parameters, radiation dose estimates, and the contrast media protocol are provided in Table 1. An automatic attenuation-based tube voltage selection was performed for optimizing and lowering the radiation dose of each CT examination. The selection is individually tailored for each patient and region to study according with the attenuation detected in the topogram. Images were acquired in craniocaudal direction with a single breath-hold for scan duration of 43 s. When this it was not possible, the patients were asked to hold breath for as long as they were capable to and then breathe superficially until the end of the examination.

Quantitative Perfusion Analysis

Processing and analysis of all data was performed on a standard workstation using dedicated software (syngo.via, VB10A, Siemens) and application (syngo.via, CT Body Perfusion, Siemens). Despite the single breath-hold protocol proposed, this is not easily executed by patients, so

Table 1 Perfusion CT and contrast media injection protocol

Parameters	
Scan width (cm)	14.8–18.2
Scan delay (s)	5
N° scans	12
Scan length (mm)	14.8–23.2
Cycle time (s)	1.5
Image thickness (mm)	4
Mean examination time (s)	43.94
Scan direction	Craniocaudal
Tube current (mAs/rot)	175/125
Tube voltage (kV)	70–100
Slice acquisition (mm)	128 × 0.6
Contrast material dosage (mL)	60
Iodine concentration (mg L/mL)	370
Dose length product (mGy × cm)	878–1030
Effective dose estimation (mSv)	32–45
Contrast flow (mL/s)	4
Contrast	Ultravist [®] , Bayer HealthCareSchering AG, Berlin, Germany

automatic motion correction and noise reduction algorithms were applied. A region of interest (ROI) was automatically placed in the abdominal aorta and was manually placed in the portal vein and the cortex of the kidney to measure the arterial and portal venous input according to the maximum slope model [21]. Color-coded parametric perfusion maps including the arterial liver perfusion (ALP, in mL/min/100 mL), portal venous liver perfusion (PLP, in mL/min/100 mL), and hepatic perfusion index (HPI, ALP/(ALP + PLP), in %) maps as well as a temporal maximum intensity projection (MIP) serving as anatomical reference were generated serving for further analysis.

Two blinded and independent readers (both with 4 years of experience in abdominal radiology) performed the perfusion measurements on the ALP maps by placing a free-hand volume of interest (VOI) covering: **A**, the central necrotic zone only (CZ); **B**, the necrotic and surrounding transition zone (TZ); and **C**, all three zones including the central necrotic, transition, and adjacent liver parenchyma/peripheral zone (PZ). Each VOI was primarily drawn on the APL map, slice by slice, until covering the entire zone (see Fig. 1). Afterward, the system automatically copied the VOIs in the same position to the PLP and HPI maps.

Statistical Analysis

Data were reviewed descriptively, and mean values with standard deviations were calculated. To evaluate the interreader agreement, intraclass correlation coefficients (ICC) were calculated for all perfusion parameters. An ICC less than 0.69 was defined as poor, ICC between 0.70 and 0.79 as fair, ICC between 0.80 and 0.89 as good, and ICC

greater than 0.9 as excellent agreement [22]. Multivariate *T* test for independent samples was performed to test for significant differences in ALP, PVP, and HPI values between complete and incomplete responders. Diagnostic accuracy of quantitative assessment for detection of early treatment response was studied with receiver operating characteristic (ROC) analysis, determining the area under the curve (AUC). *P* values <0.05 were considered statistically significant. All statistical analyses were performed using commercially available software (SPSS, release 22.0, Chicago, IL USA).

Results

Patients

P-CT was successfully performed in all 20 patients without adverse events. Except of one patient (late CM inflow), both the arterial and portal venous phases of liver perfusion could be covered in all patients. Accordingly, calculation of the ALP was successful in 20/20 (100 %) patients, whereas PLP and HPI maps were available in 19/20 (95 %) patients. Fourteen of the 20 patients (70 %) were classified as complete responders and five (30 %) as incomplete responders to RFA, according to the findings on imaging follow-up.

Perfusion CT Analysis

Interreader agreement of all perfusion parameters (ALP/PLP/HPI) was fair for the CZ (ICC, range 0.713–0.747)

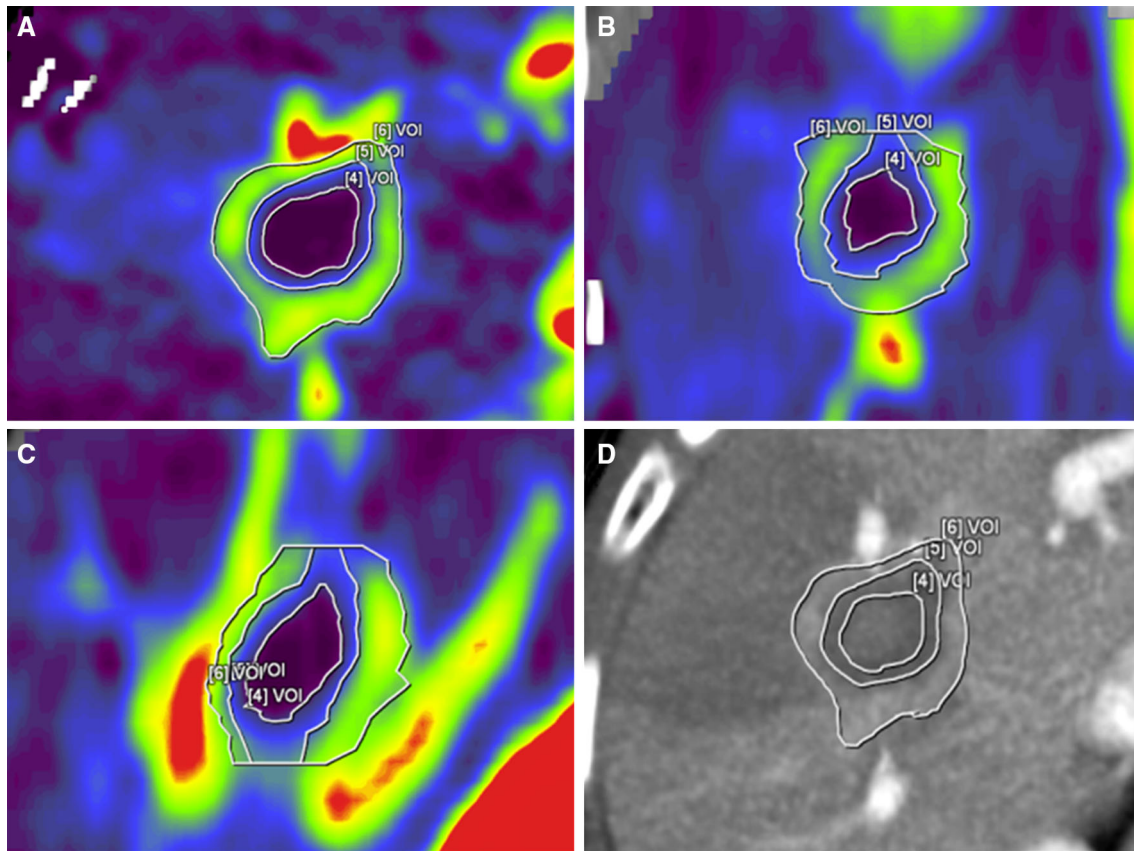


Fig. 1 A 62-year-old male patient with liver cirrhosis and HCC in segment 2 treated with RFA. Arterial liver perfusion (ALP) maps in the axial (A), coronal (B), and sagittal (C) planes were used to determine volume of interests (VOIs) within the posttreated lesion. Two readers delineated the central necrotic (VOI 4), the transition

zone (VOI 5), and the surrounding parenchymal zone (VOI 6). The three VOIs were automatically copied to the maximum intensity projection image for anatomical reference (D) as well as the venous liver perfusion and hepatic perfusion index maps (not displayed) for perfusion analysis

and good for the TZ (ICC, range 0.789–0.819). For the PZ interreader agreement was excellent for ALP (ICC, 0.941), fair for PLP (ICC = 0.701), and good for HPI (ICC = 0.858).

Mean size of treated lesions was $22.6 \text{ mm} \pm 9.3$ (range 5–35 mm). Mean ALP/PLP/HPI values (mean of both readers) were 4.5/17.2/57.2 in CZ, 8.8/18.8/62.4 in TZ, and 20.9/30.8/60.4 in PZ. Mean perfusion parameters of each reader in regard to the three ablation zones are given in Table 2.

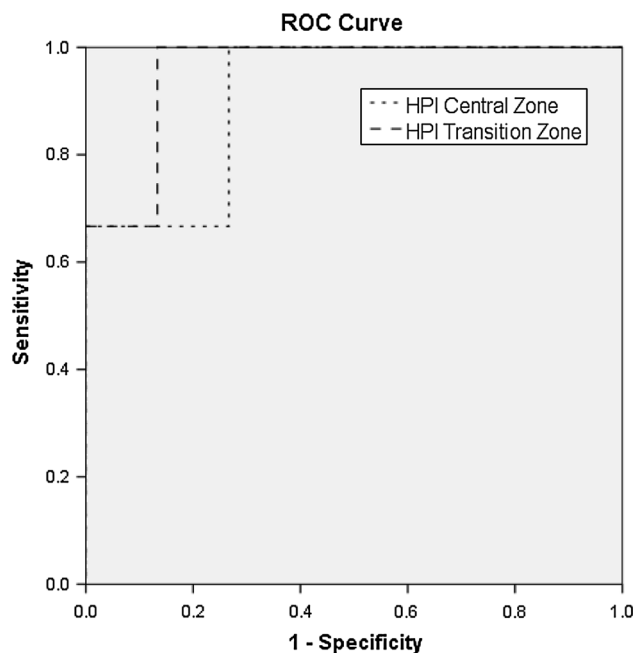
There was a significant difference between ALP ($P = 0.000$) and PLP ($P = 0.004$) but not for HPI (0.511) of the three zones (see Table 2). Both ALP and PLP were lowest in the CZ (ALP, 1.94–9.55 mL/min/100 mL; PLP, 2.92–23.27 mL/min/100 mL), and significantly higher in the TZ (ALP, 3.99–14 mL/min/100 mL; PLP, 3.32–65.49 mL/min/100 mL) and PZ (both, $P < 0.05$).

Early Treatment Assessment

Complete responders showed a mean ALP/PLP/HPI of 4.8/18.3/58.2 for the CZ, 9.9/19.5/63.4 for the TZ and 20.8/30.6/60.9 for the PZ, whereas incomplete responders showed a mean ALP/PLP/HPI of 5.2/5.6/73.6 for the CZ, 11.2/8.2/77.2 for the TZ and 21.8/25.3/65.4 for the PZ. HPI was significantly lower in complete responders as compared to incomplete responders for both the CZ and TZ (both, $P < 0.05$), whereas all other parameters showed no significant difference between the two groups (all, $P > 0.05$). ROC analysis showed an AUC for prediction of residual tumor of 0.911 (95 % CI 0.739–1) for HPI of the CZ and 0.956 (95 % CI 0.853–1) for HPI of the TZ, suggesting tumor response at a cut-off value below 73 % for the CZ and 76 % for the TZ (Fig. 2). Two representative image examples are provided in Figs. 3 and 4.

Table 2 Quantitative perfusion CT parameters of both readers derived from different tumor areas

	Central zone		Transition zone		Parenchymal zone		P value
	Reader 1	Reader 2	Reader 1	Reader 2	Reader 1	Reader 2	
	Arterial liver perfusion (mL/min/100 mL)	4.7 ± 2.6 (1.26–11.5)	4.2 ± 1.4 (2.4–7.6)	9.1 ± 4.4 (2.2–16.5)	8.5 ± 2.3 (4.7–14.2)	21.2 ± 8.5 (10.9–41.8)	
Portal liver perfusion (mL/min/100 mL)	17.4 ± 28.3 (8.3–65.1)	17.0 ± 19.5 (1.6–68.5)	19.1 ± 13.9 (9.1–27.8)	18. ± 19.2 (2.9–46.3)	30.5 ± 18.1 (15.8–35.6)	30.9 ± 17.0 (8.2–40.0)	0.044
Hepatic perfusion index (%)	55.3 ± 19.1 (7.8–80.5)	59.0 ± 15.6 (15.2–84.4)	59.9 ± 16.7 (18.6–79.3)	64.8 ± 14.3 (20.8–86.8)	59.9 ± 12.0 (45.3–74.7)	60.9 ± 13.0 (41.6–67.8)	0.511

**Fig. 2** Receiver operating characteristic (ROC) analysis of hepatic perfusion index (HPI) (central vs. transition zone) for assessment early treatment response. Univariate analysis distinction complete from incomplete responders to RFA. HPI of the central zone (CZ) and the transition zone (TZ) was the only perfusion parameter showing significant differences between complete and incomplete responders to RFA (both, $P < 0.05$). ROC analysis showed an area under the curve for depiction of residual tumor of 0.911 (95 % CI 0.739–1) for the CZ and 0.956 (95 % CI 0.853–1) for the TZ, suggesting complete response at a cut-off value below 73 % for the CZ and 76 % for the TZ

Discussion

Several studies have investigated the role of P-CT for evaluation of tumor response to various therapies in a variety of neoplasms [23, 24] including HCC [15, 16, 25–27] and liver metastases [13]. Moreover, radiation-free imaging techniques like MRI [28] and CEUS [29] have been showing promising results in regard to response evaluation to RFA. However, to the best of our knowledge, there are no data so far evaluating the treatment response to RFA immediately after therapy (within first 24 h) for both metastases and HCC. Our study shows that early treatment assessment of RFA is feasible and reproducible between different readers using the applied P-CT protocol. Except one patient with late contrast media inflow, probably due to low cardiac output, arterial and portal liver perfusion maps as well as hepatic perfusion index maps could be calculated in all patients. A total of three different perfusion zones could be distinguished on perfusion maps in both RFA-treated HCC and liver metastases, including a central necrotic, a transitional, and a peripheral/parenchymal zone. The zonal distribution

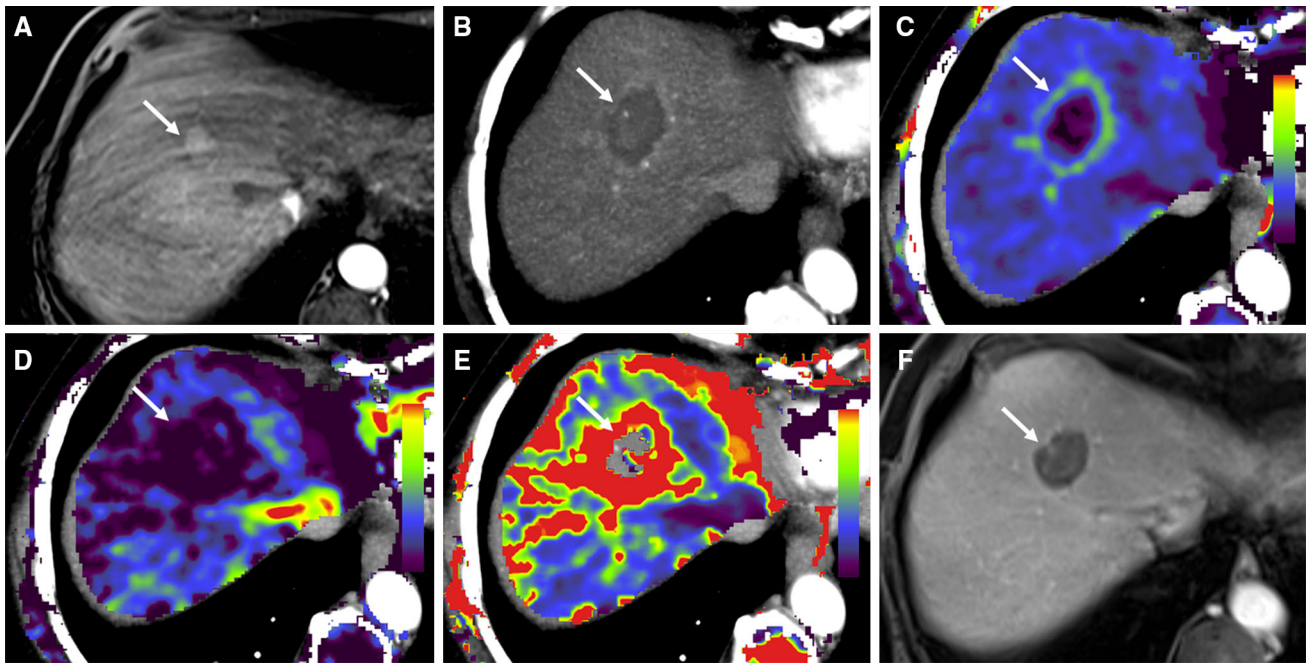


Fig. 3 A 78-year-old female patient with liver cirrhosis and HCC treated with RFA and showing complete response. Contrast-enhanced MR image performed before RFA **A** shows the arterialized HCC in liver segment 8. Maximum intensity projection of the liver **B** derived from perfusion CT (P-CT) performed 3 h after RFA shows a hypodense lesion surrounded by a thin hyperdense rim corresponding to central necrosis and surrounding reactive hyperperfusion. Arterial liver perfusion (ALP) map **C** shows no arterial perfusion in the central

zone (*dark blue*), low ALP in the transition zone (*light blue*), and hyperperfusion in the peripheral (parenchymal) zone (*light green*). The portal liver perfusion (PLP) map **D** shows the absence of PLP in all three zones, whereas the hepatic perfusion index (HPI) map **E** shows a slightly increased (*red*) HPI in the transition zone (56 %) indicating complete response (cut-off, HPI 73 %). Follow-up MR imaging 3 months after RFA **F** confirmed the P-CT diagnosis showing no residual tumor

visualized directly after treatment reflects the expected necrotic changes from the high temperature produced by alternating high-frequency current of the unipolar electrode [30]. Accordingly, ALP and PLP gradually increased from the CZ to the TZ and PZ, reflecting the differences in viable tissue. The PZ, which is not primarily treated and likely to show reactive hyperperfusion, revealed significantly higher ALP and PLP as compared to both other zones. The parallel increase of ALP and PLP in all three zones results in similar HPI values and thus in poor zonal differentiation on HPI maps.

In comparison, when evaluating residual tumor, the HPI reflecting the ratio of ALP with total tumor perfusion plays an important role in distinguishing complete from incomplete responders to local therapy. Previous studies could show that an increased HPI at greater than 1 month after treatment with TACE or RFA is suggestive for residual tumor in patients with HCC. It remains unclear, however, if P-CT at 1 month after RFA provides added value for treatment assessment compared to standard multiphase CT, which most probably provides the same or similar information on presence of residual tumor [17].

Our results are consistent with recent publications showing an increased HPI in incomplete responders to

RFA [17]. In contrast to the previous study, however, our data suggest that the increase in HPI—probably caused by the presence of residual tumor cells—can already be detected immediately after RFA using P-CT. Accordingly, HPI might serve as a biomarker for very early treatment assessment replacing standard multiphase CT or P-CT at 1 month or later after RFA [31]. Residual tumor components are most probably located in the periphery of the RFA center, which equals the “transition zone” between central total tumor necrosis and surrounding healthy liver tissue. Accordingly, our results show that HPI measurements of the TZ are best suited for early treatment assessment showing a high AUC of 0.984, slightly outperforming the AUC of the CZ (0.953). The slight differences in AUC might be due to a better interreader agreement of perfusion measurements in the TZ as compared to the CZ or the higher probability of residual tumor cells in the TZ due to the lower heat propagation to this area. In this context, our data implicate that a HPI >73 % (both, CZ and TZ) is suggestive for tumor residual or incomplete response.

To the best of our knowledge, this is the first study evaluating the interreader agreement of perfusion measurements for tumor response assessment after RFA treatment. In our study, two independent readers performed

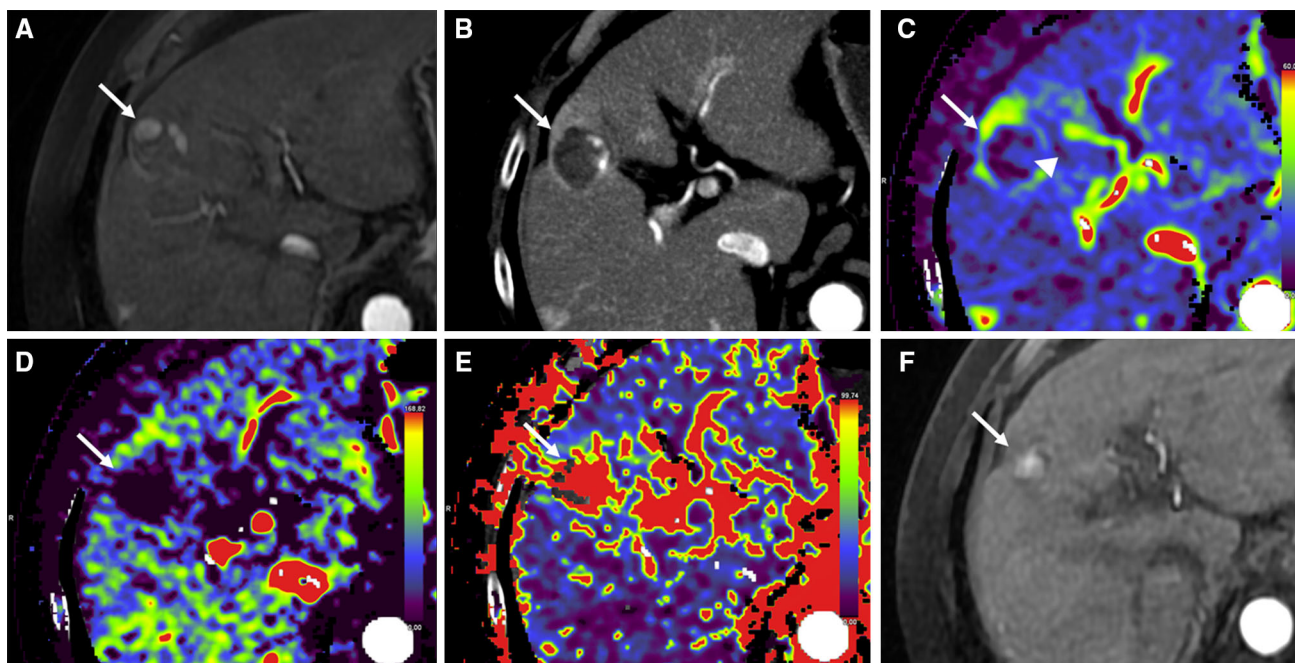


Fig. 4 A 78-year-old male patient with liver cirrhosis and a HCC in liver segment 5. Contrast-enhanced MR image performed before RFA **A** shows the arterialized HCC. Maximum intensity projection of the liver **B** derived from perfusion CT (P-CT) performed 24 h after RFA shows a hypodense lesion surrounded by a hyperdense rim corresponding to central necrosis and surrounding reactive hyperperfusion. Arterial liver perfusion (ALP) map **C** shows residual moderate ALP in the central and transition zone (arrow, light blue) and

hyperperfusion in the peripheral (parenchymal) zone (light green). The portal liver perfusion (PLP) map **D** shows the absence of PLP in all three zones, whereas the hepatic perfusion index (HPI) map **E** shows an increased (red) HPI in the central (82 %) and transition (76 %) zone indicating incomplete response (cut-off, HPI 76 and 73 %, respectively). Follow-up MR imaging 2 months after RFA **F** confirmed the P-CT diagnosis showing nodular contrast enhancement within the ablation zone consistent with residual tumor

VOI measurements of three different parenchymal zones, which could be distinguished on ALP maps. Compared to another study evaluating interreader agreement for 2D assessment of perfusion parameters in HCC in general, ICC values were substantially higher in our study (0.26–0.59 vs. 0.70–0.94) ranging from moderate to excellent depending on the zone [32]. These differences in interreader agreement are most likely related to the zonal distribution of ALP after RFA, which serves as an anatomical landmark for VOI placement as well as the 3D volumetric approach applied in our study, which does better reflect tumor inhomogeneity compared to a 2D approach. Interestingly interreader agreement was best for the PZ but still good for the TZ, which is probably related to the delineation of each zone. This is well reflected in perfusion parameters, which increase substantially from the TZ (partial necrosis) toward the PZ (reactive hyper perfusion), but show only minor differences between the central (necrotic) and the TZ.

Some limitations of our study should be acknowledged. First of all, the small number and heterogeneity of our study population consisting in patients suffering from both HCC and metastases. However, our study shows that perfusion changes seen after RFA treatment are fairly unspecific showing a zonal anatomy and ALP increase in

both tumor types. Moreover, HPI reflects the biological behavior of both HCC and metastases, which show an increased arterial blood supply in relation to the portal venous input, resulting in a relative arterialization of residual tumor components. Second, our reference standard relied on a single short-term imaging follow-up (mean 57 days), which did not allow for evaluation of long term tumor recurrence and patient survival. The large range of follow-up dates has to also be acknowledged. Finally, further prospective studies are needed to confirm our findings and the HPI cut-off value for distinguishing responders from nonresponders.

Conclusion

In conclusion, P-CT performed within 1 day after RFA of malignant focal liver lesions might allow for the quantitative assessment of zonal perfusion changes with good interreader agreement. Increased arterial perfusion of the transition zone as assessed by the hepatic perfusion index has the potential to serve as an early imaging biomarker for residual tumor. However, further studies are needed to corroborate our findings.

Compliance with Ethical Standards

Conflict of Interest The authors declare that they have no conflict of interest.

Ethical Approval All procedures performed in studies involving human participants were in accordance with the ethical standards of the institutional and/or national research committee and with the 1964 Helsinki declaration and its later amendments or comparable ethical standards.

Informed Consent Does not apply.

References

- European Association For The Study Of The L, European Organisation For R, Treatment Of C. EASL-EORTC clinical practice guidelines: management of hepatocellular carcinoma. *J Hepatol.* 2012;56(4):908–43. doi:10.1016/j.jhep.2011.12.001.
- Minami Y, Kudo M. Radiofrequency ablation of liver metastases from colorectal cancer: a literature review. *Gut Liver.* 2013;7(1):1–6. doi:10.5009/gnl.2013.7.1.1.
- Rhim H, Lim HK. Radiofrequency ablation of hepatocellular carcinoma: pros and cons. *Gut Liver.* 2010;4(Suppl 1):S113–8. doi:10.5009/gnl.2010.4.S1.S113.
- Sainani NI, Gervais DA, Mueller PR, Arellano RS. Imaging after percutaneous radiofrequency ablation of hepatic tumors: part 1, normal findings. *AJR Am J Roentgenol.* 2013;200(1):184–93. doi:10.2214/AJR.12.8478.
- Montorsi M, Santambrogio R, Bianchi P, Donadon M, Moroni E, Spinelli A et al. Survival and recurrences after hepatic resection or radiofrequency for hepatocellular carcinoma in cirrhotic patients: a multivariate analysis. *J Gastrointest Surg.* 2005;9(1):62–7; discussion 7–8. doi:10.1016/j.gassur.2004.10.003.
- Lee H, Heo JS, Cho YB, Yun SH, Kim HC, Lee WY, et al. Hepatectomy vs radiofrequency ablation for colorectal liver metastasis: a propensity score analysis. *World J Gastroenterol.* 2015;21(11):3300–7. doi:10.3748/wjg.v21.i11.3300.
- Minami Y, Nishida N, Kudo M. Therapeutic response assessment of RFA for HCC: contrast-enhanced US, CT and MRI. *World J Gastroenterol.* 2014;20(15):4160–6. doi:10.3748/wjg.v20.i15.4160.
- Kierans AS, Elazzazi M, Braga L, Leonardou P, Gerber DA, Burke C, et al. Thermoablative treatments for malignant liver lesions: 10-year experience of MRI appearances of treatment response. *AJR Am J Roentgenol.* 2010;194(2):523–9. doi:10.2214/AJR.09.2621.
- Sainani NI, Gervais DA, Mueller PR, Arellano RS. Imaging after percutaneous radiofrequency ablation of hepatic tumors: part 2, abnormal findings. *AJR Am J Roentgenol.* 2013;200(1):194–204. doi:10.2214/AJR.12.8479.
- Attenberger UI, Morelli J, Budjan J, Henzler T, Sourbron S, Bock M, et al. Fifty years of technological innovation: potential and limitations of current technologies in abdominal magnetic resonance imaging and computed tomography. *Investig Radiol.* 2015;50(9):584–93. doi:10.1097/RLI.0000000000000173.
- Fischer MA, Kartalis N, Grigoriadis A, Loizou L, Stal P, Leidner B, et al. Perfusion computed tomography for detection of hepatocellular carcinoma in patients with liver cirrhosis. *Eur Radiol.* 2015;. doi:10.1007/s00330-015-3732-1.
- Ippolito D, Sironi S, Pozzi M, Antolini L, Invernizzi F, Ratti L, et al. Perfusion CT in cirrhotic patients with early stage hepatocellular carcinoma: assessment of tumor-related vascularization. *Eur J Radiol.* 2010;73(1):148–52. doi:10.1016/j.ejrad.2008.10.014.
- Morsbach F, Sah BR, Spring L, Puipe G, Gordic S, Seifert B, et al. Perfusion CT best predicts outcome after radioembolization of liver metastases: a comparison of radionuclide and CT imaging techniques. *Eur Radiol.* 2014;24(7):1455–65. doi:10.1007/s00330-014-3180-3.
- Reiner CS, Morsbach F, Sah BR, Puipe G, Schaefer N, Pfammatter T, et al. Early treatment response evaluation after yttrium-90 radioembolization of liver malignancy with CT perfusion. *J Vasc Interv Radiol.* 2014;25(5):747–59. doi:10.1016/j.jvir.2014.01.025.
- Ippolito D, Bonaffini PA, Ratti L, Antolini L, Corso R, Fazio F, et al. Hepatocellular carcinoma treated with transarterial chemoembolization: dynamic perfusion-CT in the assessment of residual tumor. *World J Gastroenterol.* 2010;16(47):5993–6000.
- Sabir A, Schor-Bardach R, Wilcox CJ, Rahmanuddin S, Atkins MB, Kruskal JB, et al. Perfusion MDCT enables early detection of therapeutic response to antiangiogenic therapy. *AJR Am J Roentgenol.* 2008;191(1):133–9. doi:10.2214/AJR.07.2848.
- Ippolito D, Fior D, Bonaffini PA, Capraro C, Leni D, Corso R, et al. Quantitative evaluation of CT-perfusion map as indicator of tumor response to transarterial chemoembolization and radiofrequency ablation in HCC patients. *Eur J Radiol.* 2014;83(9):1665–71. doi:10.1016/j.ejrad.2014.05.040.
- Bruix J, Sherman M. American association for the study of liver D. Management of hepatocellular carcinoma: an update. *Hepatology.* 2011;53(3):1020–2. doi:10.1002/hep.24199.
- Bruix J, Sherman M, Llovet JM, Beaugrand M, Lencioni R, Burroughs AK, et al. Clinical management of hepatocellular carcinoma. Conclusions of the Barcelona-2000 EASL conference. European association for the study of the liver. *J Hepatol.* 2001;35(3):421–30.
- Goetti R, Leschka S, Desbiolles L, Klotz E, Samaras P, von Boehmer L, et al. Quantitative computed tomography liver perfusion imaging using dynamic spiral scanning with variable pitch: feasibility and initial results in patients with cancer metastases. *Investig Radiol.* 2010;45(7):419–26. doi:10.1097/RLI.0b013e3181e1937b.
- Fischer MA, Brehmer K, Svensson A, Aspelin P, Brismar TB. Renal versus splenic maximum slope based perfusion CT modelling in patients with portal-hypertension. *Eur Radiol.* 2016;. doi:10.1007/s00330-016-4277-7.
- Landis JR, Koch GG. The measurement of observer agreement for categorical data. *Biometrics.* 1977;33(1):159–74.
- Hayano K, Fujishiro T, Sahani DV, Satoh A, Aoyagi T, Ohira G, et al. Computed tomography perfusion imaging as a potential imaging biomarker of colorectal cancer. *World J Gastroenterol.* 2014;20(46):17345–51. doi:10.3748/wjg.v20.i46.17345.
- Preda L, Calloni SF, Moscatelli ME, Cossu Rocca M, Bellomi M. Role of CT perfusion in monitoring and prediction of response to therapy of head and neck squamous cell carcinoma. *Biomed Res Int.* 2014;2014:917150. doi:10.1155/2014/917150.
- Chen G, Ma DQ, He W, Zhang BF, Zhao LQ. Computed tomography perfusion in evaluating the therapeutic effect of transarterial chemoembolization for hepatocellular carcinoma. *World J Gastroenterol.* 2008;14(37):5738–43.
- Kan Z, Phongkitkarun S, Kobayashi S, Tang Y, Ellis LM, Lee TY, et al. Functional CT for quantifying tumor perfusion in antiangiogenic therapy in a rat model. *Radiology.* 2005;237(1):151–8. doi:10.1148/radiol.2363041293.
- Zhu AX, Holalkere NS, Muzikansky A, Horgan K, Sahani DV. Early antiangiogenic activity of bevacizumab evaluated by computed tomography perfusion scan in patients with advanced hepatocellular carcinoma. *Oncologist.* 2008;13(2):120–5. doi:10.1634/theoncologist.2007-0174.

28. Chapiro J, Duran R, Lin M, Scherthaner R, Lesage D, Wang Z, et al. Early survival prediction after intra-arterial therapies: a 3D quantitative MRI assessment of tumour response after TACE or radioembolization of colorectal cancer metastases to the liver. *Eur Radiol.* 2015;25(7):1993–2003. doi:[10.1007/s00330-015-3595-5](https://doi.org/10.1007/s00330-015-3595-5).
29. Bartolotta TV, Taibbi A, Matranga D, Midiri M, Lagalla R. 3D versus 2D contrast-enhanced sonography in the evaluation of therapeutic response of hepatocellular carcinoma after locoregional therapies: preliminary findings. *Radiol Med.* 2015;120(8):695–704. doi:[10.1007/s11547-015-0514-4](https://doi.org/10.1007/s11547-015-0514-4).
30. Decadt B, Siriwardena AK. Radiofrequency ablation of liver tumours: systematic review. *Lancet Oncol.* 2004;5(9):550–60. doi:[10.1016/S1470-2045\(04\)01567-0](https://doi.org/10.1016/S1470-2045(04)01567-0).
31. Lim HK, Choi D, Lee WJ, Kim SH, Lee SJ, Jang HJ, et al. Hepatocellular carcinoma treated with percutaneous radio-frequency ablation: evaluation with follow-up multiphase helical CT. *Radiology.* 2001;221(2):447–54. doi:[10.1148/radiol.2212010446](https://doi.org/10.1148/radiol.2212010446).
32. Ippolito D, Casiraghi AS, Talei Franzesi C, Bonaffini PA, Fior D, Sironi S. Intraobserver and interobserver agreement in the evaluation of tumor vascularization with computed tomography perfusion in cirrhotic patients with hepatocellular carcinoma. *J Comput Assist Tomogr.* 2016;40(1):152–9. doi:[10.1097/RCT.0000000000000331](https://doi.org/10.1097/RCT.0000000000000331).